Microsyenite from Lake Mykle, Oslo Rift: Subvolcanic rocks transitional between larvikite and nordmarkite

TOM ANDERSEN & HENNING SØRENSEN

Andersen, T. & Sørensen, H. 2003: Mikrosyenite from Lake Mykle, Oslo Rift: Subvolcanic rocks transitional between larvikite and nordmarkite. *Norges geologiske undersøkelse Bulletin 441,* 25–31.

A small body of trachyte or microsyenite cropping out east of lake Mykle in the Vestfold Graben of the Oslo Rift probably represents a subvolcanic intrusion emplaced at a fairly early stage of the intrusive history of the Siljan-Mykle area. The microsyenite shows chemical, petrographical and mineralogical features intermediate between larvikite and nordmarkite, suggesting that it represents a transitional magma type. The microsyenite shows pyroxene zonation patterns indicating a discontinuous, two-stage crystallization history, whose initial stage resembles that observed in normal larvikite. At the final stage of pyroxene growth, the melt had developed to a more alkaline composition, resembling some of the less alkaline (alkali)syenites in the rift.

Tom Andersen, Institutt for geofag, Universitetet i Oslo, Postboks 1047 Blindern, N-0316 Oslo, Norge. Henning Sørensen, Geologisk Institut, Københavns Universitet, Øster Voldgade 10, DK-1350 København K, Danmark

Introduction

The Oslo Rift igneous province in Southeast Norway consists of large plateaus of volcanic rocks, major plutonic complexes, cauldron structures and a multitude of dykes. At the present level of exposure, the predominant volcanic rocks are the well-known rhomb porphyries which are characterised by rhomb-shaped phenocrysts of anorthoclase feldspar. They range in composition from tephri-phonolite to trachyandesite/latite and correspond chemically and mineralogically to the plutonic rock larvikite. Basalts are relatively less abundant. In spite of the widespread occurrence of nordmarkite and other types of syenites in the Oslo Rift, trachytic lava is a rare rock type, only found associated with cauldrons (e.g., Oftedahl & Petersen 1978). In the present paper, we report the discovery of a small body of subvolcanic trachyte or microsyenite on the east coast of lake Mykle in the southwestern part of the Oslo Rift, in a region underlain by plutonic larvikite, syenites and granites; its distance to exposed volcanic rocks is about 10 km (Fig. 1). This occurrence of microsyenite is briefly described, and its petrogenetical relationship to the major plutonic rock types of the province is evaluated from whole-rock and mineral compositions.

Field occurrence

The area around lake Mykle (Fig. 1) forms part of the 1:50 000 geological map-sheet Siljan, and is characterised by the occurrence of a considerable variety of plutonic igneous rocks, which is an indication that this part of the Oslo igneous province has been the site of intensive igneous activity during long periods. It is dominated by large plutons of larvikite which are exposed to the north and south of the lake. In the western part of the area, the highest parts of the landscape are made up of larvikite forming the roof of granite and syenite intrusions. This indicates that larvikite may originally have formed one continuous body, which is now separated by large intrusive masses of granite and minor masses of syenite, that form the landscape around the lake. In the central part of the map-sheet the highest peaks are composed of granite.

Geological mapping of the Siljan map-sheet, carried out by staff and students from the Geological Institute, University of Copenhagen, has established the following succession of magmatic events in the Mykle area:

1. *Larvikite*, making up a large pluton which was most probably formed by several intrusive events.
2. Intrusion of small bodies of *gabbro/diorite* (Pedersen 1994, Pedersen & Sørensen 2003) and nepheline syenite (Andersen & Sørensen 1993). The gabbro contains xenoliths of larvikite, and the larvikite is intersected by dykes of nepheline syenite, showing that the gabbros and nepheline syenites are younger than the larvikite. The gabbro and the nepheline syenite are intruded by syenite and granite. Their mutual age relationship is unknown.
3. Intrusion of small bodies of *porphyritic syenite* (Petersen & Sørensen 1997) which contain xenoliths of larvikite and gabbro but are intersected by several generations of dykes of syenite and granite.
4. Bodies of *syenite* (nordmarkite) and granite which intersect the porphyritic syenite. They contain net-veined complexes in their contact zones with larvikite (Morogan & Sørensen 1994).
5. A large body of coarse-grained *alkali granite* of ekeritic type (Brøgger 1906).

The microsyenite described in the present paper is located on the east coast of lake Mykle where it forms the southern contact of the ekeritic granite. It is the only exam-

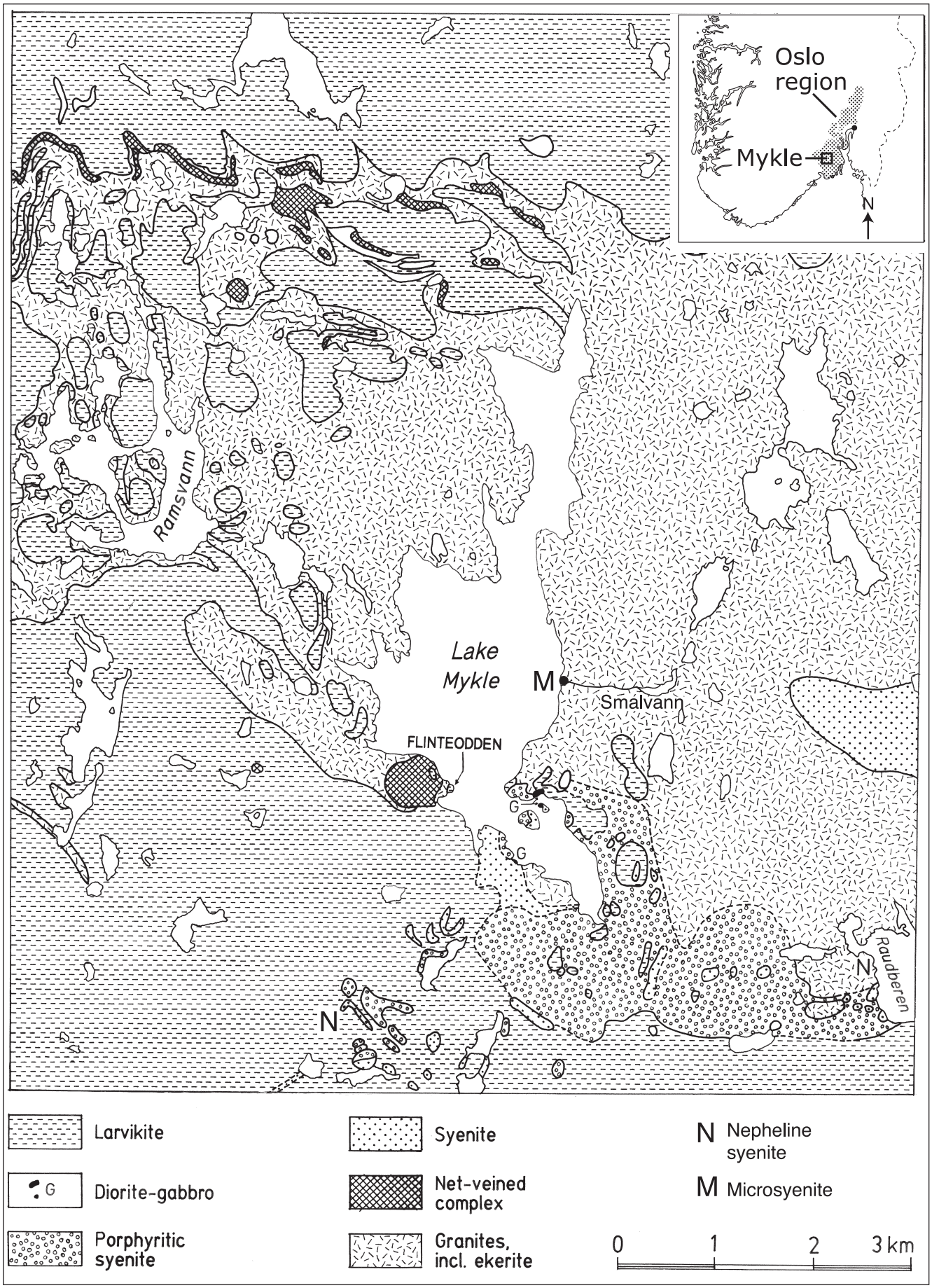
Oslo region
Mykle
N
Ramsvann
Lake Mykle
M
Smålvann
FLINTEODDEN
G
G
N
N
Raudberen
Larvikite
Diorite-gabbro
Porphyritic syenite
Syenite
Net-veined complex
Granites, incl. ekerite
N Nepheline syenite
M Microsyenite
0 1 2 3 km

Fig. 2. The outcrop of microsyenite along the forest road on the east coast of Mykle. Note the pronounced horizontal sheet jointing in the microsyenite.

Fig. 3. Coarse-grained ekerite intruding microsyenite along horizontal sheet jointing.

ple of its kind recorded in the area. It is older than this granite but its age relations to the other intrusive rocks are unknown. The microsyenite is exposed along the forest road on the west coast of Mykle (UTM reference 5394 65893) for a distance of about 200 m to the south and north of the bridge over Smalvannelva (Fig. 1). At the northern end of the exposure, the microsyenite is in contact with ekeritic granite and is intruded by sheets of ekerite and pegmatite (Fig. 2) along horizontal sheet jointing of the microsyenite (Fig. 3). The boundaries of the microsyenite towards the east, south and west are concealed under a cover of vegetation and loose deposits. The shape and size of the microsyenite body are therefore unknown, and it cannot be decided from field evidence if it represents remnants of a dyke, plug or lava flow. Over a distance of about 100 m to the north of the contact, the granite contains numerous angular to rounded xenoliths of microsyenite up to about 30 cm across. The veins of granite and pegmatite intersecting the microsyenite are highly miarolitic.

Fig. 1. Simplified geological map of the Mykle area, from the northwestern part of the 1:50,000 map-sheet Siljan.

Petrography

The microsyenite is white and fine-grained, with an average grain size < 1 mm, but with scattered larger grains of alkali feldspar attaining 2-3 mm in size. The predominant mineral of the microsyenite is alkali feldspar (≥95 %) occurring as rectangular grains which only exceptionally show weakly developed cross-hatched microcline twinning. Some of the larger grains of alkali feldspar have cores of plagioclase similar to the feldspars of larvikite and rhomb porphyry. The platy alkali feldspar grains have rims of albite and vesicles are surrounded by plates of albite. The texture is interlocking without any preferred orientation of the feldspars. There are scattered grains of green clinopyroxene and more rare bluish amphibole, the latter in places with cores of clinopyroxene. Accessory minerals are titanite, sometimes with cores of ilmenite, Fe-Ti oxides and apatite. Brownish grains are most probably allanite. The feldspar, pyroxene and amphibole grains are practically unaltered in some samples, but the feldspar grains become turbid and the pyroxenes and amphibole are altered into biotite and rust-coloured material in some thin-sections. Some samples also have plates of biotite. In one thin-section, there is a little interstitial quartz associated with biotite, and secondary muscovite, chlorite and calcite.

The intruding alkali granite is coarse-grained and composed of perthitic alkali feldspar, quartz and some interstitial albite. Aggregates of biotite, chlorite and Fe-Ti oxides are most probably formed by alteration of the original pyroxene and amphibole. Accessories are zircon as crystals and irregularly shaped grains, titanite and pyrochlore.

Mineral chemistry

Pyroxenes and amphiboles in samples 86062 and 23354 were analysed by electron microprobe, using a five-spectrometer CAMECA SX100, wavelength-dispersive instrument at the Department of Geosciences, University of Oslo. Grains were imaged by backscattered electrons prior to analysis.

Pyroxene

The pyroxenes in 86062 and 23354 have pale green and weakly pleochroic cores surrounded by grass-green rims. The rims are bright in backscattered electrons, and the core-rim interface is in general, quite sharp but irregular, which suggests that the cores have grown as skeletal grains, or that they have been resorbed prior to crystallization of the rims (Fig. 4). Selected analyses are given in Table 1. The full set of data can be obtained from the authors on request.

The pyroxene cores are sodic augites/salites comparable in composition to pyroxenes in larvikite from the Oslo Rift (Neumann 1976), whereas the rims plot along a trend towards Ac (Fig. 5). The maximum Ac-enrichment observed in the outer rims is 55%, but most analysed points give Ac well below 50%. The level of Hd enrichment along this trend is similar to what has been observed in peralkaline syenites

Table 1. Selected analyses of clinopyroxene and amphibole.

Sample	86062								23354						23354		
Point	HS1-1-4	HS1-1-5	HS1-1-6	HS1-1-7	HS1-5-1	HS1-5-3	HS1-5-4	HS2-3-6	HS2-3-8	HS2-4-3	HS2-4-4	HS2-4-5	HS2-4-6	HS2-1-1b	HS2-1-2	HS2-1-2b	HS2-1-2c
Mineral	Clinopyroxene							Clinopyroxene						Amphibole			
					core	c/r interface	rim		rim		green rim	pale zone	tip	Green	Blue	Blue	Blue
SiO_2	52.23	52.33	51.55	51.37	52.79	51.08	51.14	52.34	50.86	51.13	51.67	51.41	51.53	52.68	50.06	50.35	50.80
Al_2O_3	1.24	1.19	0.34	0.28	0.56	0.43	0.29	0.98	0.21	1.96	0.32	1.59	0.49	0.72	0.86	0.72	0.76
TiO_2	0.45	0.40	0.17	0.18	0.34	0.16	0.21	0.36	0.00	0.74	0.17	0.58	0.25	0.52	0.28	0.21	0.22
FeO	10.79	10.31	22.14	22.25	12.12	18.81	22.83	11.32	22.66	10.32	22.49	10.87	17.41	24.04	33.45	33.38	33.54
MgO	11.63	12.12	4.27	4.13	11.07	6.14	3.73	11.09	2.70	11.72	3.59	11.46	6.55	6.93	1.15	1.19	1.53
MnO	0.93	0.89	2.15	2.18	1.93	2.37	2.18	1.03	2.31	0.60	2.58	0.67	1.76	2.48	1.62	1.83	1.84
CaO	22.13	22.48	14.43	13.77	20.13	18.37	13.37	22.17	17.63	22.69	13.17	22.84	18.97	7.96	2.19	2.02	2.69
Na_2O	1.05	1.05	4.95	5.43	1.45	2.92	5.63	1.20	3.16	1.03	5.51	1.04	2.79	2.82	5.43	5.73	5.40
K_2O	0.00	0.00	0.01	0.00	0.00	0.00	0.01	0.04	0.01	0.00	0.01	0.00	0.02	0.44	0.77	0.64	0.75
Total	100.45	100.76	100.01	99.59	100.39	100.27	99.38	100.53	99.53	100.19	99.50	100.45	99.77	98.58	95.80	96.07	97.52
Si	1.954	1.946	1.985	1.981	1.985	1.966	1.979	1.961	2.013	1.913	2.000	1.923	1.985	7.922	7.904	7.925	7.885
Al	0.055	0.052	0.016	0.013	0.025	0.019	0.013	0.043	0.010	0.086	0.014	0.070	0.022	0.127	0.160	0.133	0.138
Ti	0.013	0.011	0.005	0.005	0.010	0.005	0.006	0.010	0.000	0.021	0.005	0.016	0.007	0.058	0.033	0.025	0.026
Fe^{3+}	0.089	0.110	0.373	0.421	0.090	0.257	0.441	0.104	0.207	0.121	0.389	0.127	0.203	0.441	1.407	1.412	1.375
Fe^{2+}	0.249	0.210	0.340	0.297	0.291	0.348	0.298	0.251	0.543	0.202	0.339	0.213	0.358	2.583	3.010	2.981	2.979
Mg	0.648	0.672	0.245	0.238	0.621	0.352	0.215	0.619	0.159	0.654	0.207	0.639	0.376	1.553	0.271	0.280	0.355
Mn	0.029	0.028	0.070	0.071	0.062	0.077	0.072	0.033	0.077	0.019	0.085	0.021	0.057	0.315	0.216	0.244	0.242
Ca	0.887	0.895	0.595	0.569	0.811	0.758	0.554	0.890	0.748	0.910	0.546	0.915	0.783	1.282	0.371	0.340	0.447
Na	0.076	0.076	0.369	0.406	0.105	0.218	0.423	0.087	0.243	0.075	0.414	0.075	0.208	0.822	1.663	1.748	1.625
K	0.000	0.000	0.000	0.000	0.000	0.000	0.001	0.002	0.001	0.000	0.000	0.000	0.001	0.085	0.156	0.128	0.148
NaB														0.718	1.629	1.660	1.553
(Na+K)A														0.189	0.189	0.216	0.219

Weight percent oxides by electron microprobe analysis. Structural formulae have been calculated on the basis of 4 cations for pyroxene, and Si+Al+Ti+Fe+Mg+Mn=13 for amphibole.

Fe^{3+} has been estimated from stoichiometric charge balance to 4 oxygen for pyroxene and 46 negative charge units for amphibole.

and granites from the Oslo Rift (Neumann 1976, Andersen 1984), but does not reach the strongly Ac-enriched compositions (Ac≥ 90%) seen in peralkaline syenites and granites in the rift (Neumann 1976). It should be noted that the pyroxene trend is not continuous, but shows a distinct compositional break between core and rim compositions.

The substitution mechanisms of the pyroxenes are illustrated in Fig. 6. The composition of the cores is controlled by

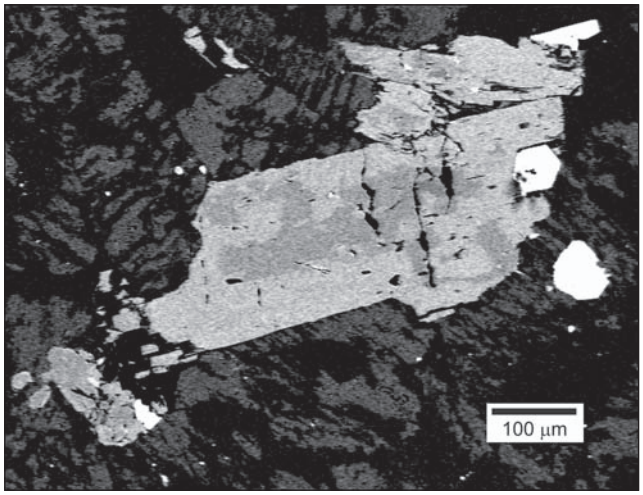

Fig. 4. Electron backscatter image of pyroxene (grey) with magnetite (white) in perthitic feldspar matrix (dark) in sample 8602. The dark grey, skeletal or resorbed core in the pyroxene (analysis HS1-5-1) consists of Ac-poor pyroxene, and the backscatter bright rim or overgrowth of aegirine-augite is zoned towards increasing Ac (analysis HS1-5-4)

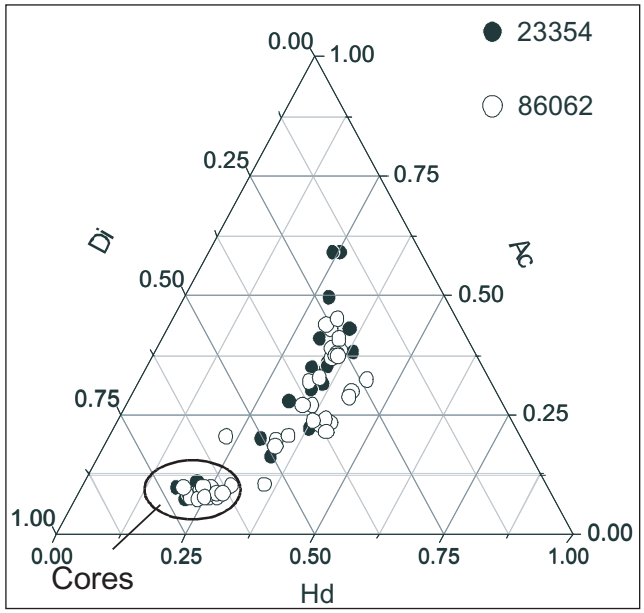

Fig. 5. Pyroxene compositions plotted in the Di-Hd-Ac plane.

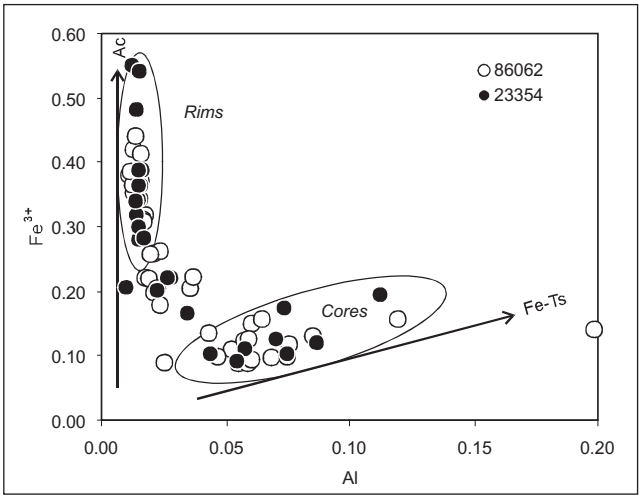

Fig. 6. Plot of total calculated Fe^{3+} and Al in clinopyroxene, with arrows representing the acmite ($Mg_{M1}Ca_{M2}=Fe^{3+}{}_{M1}Na_{M2}$) and ferri-tschermak ($Mg_{M1}Si_{T}=Fe^{3+}{}_{M1}Al_{T}$) substitutions.

the Fe-Ts substitution ($Fe^{3+}{}_{M1}$ + Al_T), and the rims by the Ac substitution (Na_{M2}+$Fe^{3+}{}_{M1}$).

Amphibole

Amphibole is absent from 86062, and is sparsely present in 23354, where it occurs as blue to green pleochroic grains intergrown with pyroxene. Selected analyses are given in Table 1. The amphiboles range in composition from ferrorichterite to riebeckite with $(Na+K)_A < 0.5$. In contrast, most plutonic sodic and sodic-calcic amphiboles from the Oslo Rift have higher A-site occupancies, ranging from sodic edenite to magnesioarfvedsonite/arfvedsonite (Neumann 1976, Andersen 1984).

Table 2. Major element compositions of microsyenite and comparable rocks.

	Ekerite	Microsyenite		Trachyte	Syenite
	86060	86062	86064	(T1)*	81462**
		Weight percent oxides			
SiO_2	76.95	64.33	62.58	64.30	60.80
TiO_2	0.24	0.62	0.69	1.10	1.27
Al_2O_3	10.94	17.05	18.13	14.17	15.83
Fe_2O_3	1.65	2.60	3.38	3.79	2.40
FeO	0.52	1.21	0.66	1.00	3.45
MnO	0.12	0.13	0.15	0.12	0.15
MgO	n.d.	0.39	0.48	1.30	1.31
CaO	0.18	1.57	1.28	1.40	2.29
Na_2O	3.99	5.90	6.68	5.68	5.05
K_2O	4.78	5.18	4.88	3.60	5.33
P_2O_5	n.d.	0.13	0.26	n.d.	0.42
H_2O+	0.23	0.33	0.49	0.35	0.86
H_2O-	0.12	0.18	0.25	0.09	n.d.
Sum	99.72	99.62	99.91	96.9	99.16
		CIPW norm. weight percent			
qz	36.01	7.11	2.36	13.52	5.05
co	0.00	0.00	0.16	0.00	0.00
or	28.24	30.60	28.83	21.27	31.49
ab	29.66	49.90	56.49	48.04	42.71
an	0.00	4.75	4.65	2.55	4.80
ac	3.60	0.00	0.00	0.00	0.00
di	0.80	1.86	0.00	3.58	3.24
hs	0.02	0.22	1.38	1.82	4.54
ilm	0.46	1.18	1.31	2.09	2.41
mt	0.59	2.53	0.62	0.43	3.48
ap	0.00	0.31	0.62	0.00	0.99
P.I.	1.07	0.90	0.90	0.93	0.89
D.I.	93.91	87.61	87.68	82.83	79.25

Whole-rock chemistry

Two samples of microsyenite (86062, 86064) and one sample of the intruding granite (86060) have been analysed for major and trace elements (Tables 2 and 3). Major element analyses were made by XRF at the Laboratoire de Pétrographie et Volcanologie, Université de Paris Sud, Orsay, France (Mme. R. Coquet); trace elements at the Geological Institute, University of Copenhagen by XRF (J.C. Bailey) and at Tracechem A/S by INAA (R. Gwozdz). Additional data for a T1 trachyte flow from the Vestfold plateau c. 30 km ENE of Mykle (Oftedahl & Petersen 1978), and a syenite (81462) from the west coast of Lake Mykle (Petersen & Sørensen 1997) are given for comparison.

Sample 86064 is weakly miarolitic, which may explain its elevated Na_2O and Cl. Otherwise, there is practically no difference in chemistry between the two samples. The chondrite-normalised REE diagram shows a rather steep slope in

Table 3. Trace element concentrations (ppm), whole rocks.

	Ekerite	Microsyenite		Syenite
	86060	86062	86064	81462**
Li	45	10	n.d.	n.a.
Cs	4.2	0.8	3.7	4.8
Rb	220	135	195	250
Be	8	7	n.d.	n.a.
Ba	36	1440	n.a.	700
Pb	12	9	n.a.	18
Sr	22	748	779	216
Zr	669	581	488	1630
Hf	25.7	14	10.9	39.6
Nb	203	182	136	205
Ta	14.7	10.8	10.2	13.6
V	3	22	n.a.	38
Ni	7	7	n.a.	5
Sc	2.3	2.3	2.5	9.5
Ga	34	28	n.a.	28
Zn	118	158	135	103
Cr	3	2.6	3.1	5
La	42.6	104	119	148
Ce	101	188	200	300
Nd	49	76	78	127
Sm	11.8	10.5	10.8	19.4
Eu	1.5	2.4	2.7	3.5
Tb	2.9	1.6	1.6	3
Yb	8.4	5.6	4.3	9.5
Lu	1.3	0.9	0.6	1.4
Y	101	59	n.a.	90
Th	16	25	26	56
U	9.6	7.6	7.5	12

**: West coast of lake Mykle
n.a: Not analysed n.d.: Below detection limit

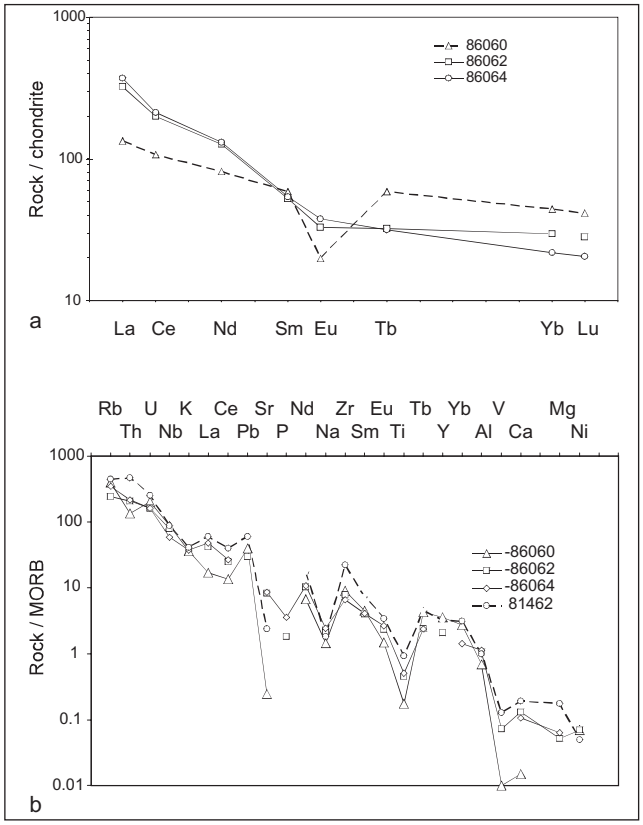

Fig. 7. (a). Chondrite-normalised REE diagram of microsyenite (86062 and 86064) and granite (86060). Chondrite data from Boynton (1984). (b) Spider diagram, normalised to N-MORB. MORB data from Wood (1979).

the LREE part and an almost horizontal HREE part of the diagram (Fig. 7a). Contrary to the granite of the area, which has marked, negative Eu anomalies, the microsyenite shows very weak or non-existing Eu anomalies, as is also the case for larvikite and syenites of the Mykle area (Petersen & Sørensen 1997). Contrary to ekerite, the Mykle microsyenite is not peralkaline; its peralkalinity index is 0.90, similar to the indices of the syenite from lake Mykle and the trachyte from the Vestfold plateau (Table 2). The syenite at lake Mykle has distinctly higher contents of LREE, Th and Zr than the microsyenite (Table 3, Fig. 7b), which is also slightly lower in SiO_2, Al_2O_3 and Na_2O and higher in CaO and TiO_2. The T1 trachyte is slightly richer in femic components and slightly poorer in the alkali feldspar components than the Mykle microsyenite.

Discussion

The lack of exposures prevents determination of the shape and size of the microsyenite body at lake Mykle. The fine grain size combined with the size of the outcrop makes a plutonic origin highly unlikely. The shape of the outcrop does not indicate a dyke- or sheet-like form for the microsyenite body. The even-grained, holocrystalline nature of the rock, and the absence of trachytic texture makes an origin as a lava flow highly unlikely. The best interpretation of the microsyenite is therefore that it is a remnant of a subvolcanic body of trachyte, which most probably belongs to stage 2 of the intrusive history of the Mykle area. Apart from pigmentation of the feldspar, rust-coloration of pyroxene and amphibole, and the rare occurrence of quartz, biotite and muscovite, the microsyenite does not appear to have been contact-metasomatised by the ekeritic granite emplaced in stage 5.

The few trachytic lavas known from the Oslo igneous province are associated with cauldron structures, which are deep sections through evolved central volcanoes (Oftedahl & Petersen 1978, Ramberg & Larsen 1978). Taking into consideration that the primary contact relationships of the diverse rock types formed during stage 2 have been obliterated by younger intrusions, we cannot exclude the former presence of a central volcano at this stage. In any case, our observations add one more type of igneous rock to the variety of igneous rocks in the complicated contact zone between the northern granite and the southern larvikite exposed on the east coast of Mykle. Most of this area is covered by forest, and the relationship between the various rock types can only be unravelled where the bedrock is exposed along lakes, roads and rivers. It is therefore possible that trachytic rocks are more widespread in the region, but concealed beneath vegetation and loose deposits.

In terms of major and trace element composition, the Mykle microsyenite is less evolved than the nordmarkite intrusions in the Oslo Rift. Its REE distribution pattern resembles larvikite more than any other rock types from the region (cf. Neumann 1980). The compositional evolution of the pyroxenes is discontinuous, with cores resembling pyroxenes in larvikite, overgrown by pyroxene trending towards the sodic compositions seen in nordmarkite and ekerite, but without reaching the extreme compositions observed in the most evolved alkaline plutons (cf. Neumann 1976, Andersen 1984). The core-rim relationships of the pyroxene suggest two distinct stages of crystal growth, the first of which involved growth of augitic pyroxene, and the later of alkaline pyroxene. The irregular core-rim interfaces suggest that these processes were separated by a stage of resorption.

The larvikites in the Oslo Rift formed by polybaric differentiation of a mafic parent magma, with an initial stage of evolution in magma chambers in the deep to middle crust (Neumann 1980), but pyroxenes and amphiboles formed at a late stage of evolution, more or less in situ (Neumann 1976). In nordmarkite and ekerite, mafic silicates are late-stage, interstitial phases which grew in situ (Neumann 1976, Andersen 1984). The first stage of pyroxene growth in the Mykle microsyenite may be related to the fractionation of a larvikite-like magma during transport to the shallow crust. An initial, larvikite-related stage of evolution is also suggested by the presence of cored feldspars. While ponded in a shallow magma chamber, this melt must have developed towards more alkaline compositions than those observed in

larvikite and related rocks. This may be due to continued fractional crystallization, or to mixing with a more evolved magma. If magma mixing is the reason, homogenization of the mixed magma must have been essentially complete, and must have taken place before final emplacement of the magma.

Conclusions

The microsyenite on the eastern shore of Lake Mykle may have been formed during stage 2 of the evolution of the Mykle magmatic complex, which also comprises emplacement of gabbro and nepheline syenite. The primary structural relationships of the rocks formed at this stage were obliterated by later, voluminous syenite and granite intrusions. The most likely origin of the microsyenite is as a shallow, subvolcanic intrusion, possibly related to the eruption of no longer preserved trachytic lavas. In terms of major and trace element composition, the Mykle microsyenite is intermediate in composition between larvikite and nordmarkite. Pyroxene and feldspar zonation patterns suggest that the trachytic magma developed through two distinct stages of evolution. The Mykle microsyenite is therefore a transitional rock type in the Oslo Rift, representing either a cogenetic 'missing link' between larvikitic and nordmarkitic trends of evolution, or a well-homogenized hybrid between the two.

Acknowledgements

The field and laboratory investigations of HS were supported by the Geological Survey of Norway, the Danish Natural Science Research Council and the Carlsberg Foundation. We are grateful for analytical work provided by Mme. R. Coquet, Université de Paris-Sud, Dr. J.C. Bailey, University of Copenhagen and Dr. R. Gwozdz, Tracechem A/S, Copenhagen; and to Dr. Muriel Erambert, University of Oslo for assistance in the electron microprobe lab. Britta Munck and Ole Bang Berthelsen, University of Copenhagen, assisted with the preparation of illustrations. Thanks are due to Prof. E.-R. Neumann and Dr. B. Sundvoll, University of Oslo, for comments and helpful suggestions, and to Odd Nilsen and Tore Prestvik for helpful reviews.

References

Andersen, T. 1984: Crystallization history of a Permian composite monzonite-alkali syenite pluton in the Sande Cauldron, Oslo Rift. *Lithos 17,* 153–170

Andersen, T. & Sørensen, H. 1993: Crystallization and metasomatism of nepheline syenite xenoliths in quartz-bearing intrusive rocks in the Permian Oslo rift, SE Norway. *Norsk Geologisk Tidsskrift 73,* 250–266.

Boynton, W.V. 1984: Cosmochemistry of the rare earth elements. Meteorite studies. *In: Rare Earth Element Geochemistry, Developments in Geochemistry 2,*. Elsevier, Amsterdam, 63–114

Brøgger, W.C. 1906: Eine Sammlung der wichtigsten Typen der Eruptivgesteine des Kristianiagebietes nach ihren geologischen Verwandschaftsbeziehungen geordnet. *Nyt Magazin for Naturvidenskaberne 44/2*, 113–144.

Morogan, V. & Sørensen, H. 1994: Net-veined complexes in the Oslo Rift, southeast Norway. *Lithos 32,* 21–45.

Neumann, E.-R. 1976: Compositional relations among pyroxenes, amphiboles and other mafic phases in the Oslo region plutonic rocks. *Lithos 9,* 85-109

Neumann E.-R. 1980: Petrogenesis of the Oslo region larvikites and associated rocks. *Journal of Petrology 21*, 499–531.

Oftedahl, C. & Petersen, J.S. 1978: Southern part of the Oslo Rift. In: Dons, J.A. & Larsen, B.T. (eds.): The Oslo Paleorift. A review and guide to excursions. *Norges geologiske undersøkelse 337,* 163–182.

Pedersen, L. 1994: *En petrologisk. mineralogisk og geokemisk undersøgelse af en gabbroisk-dioritisk-monzodioritisk intrusion ved søen Mykle, Oslofeltet, SØ Norge* (in Danish). Unpublished cand. scient. dissertation, Geological Institute, University of Copenhagen.

Pedersen, L. & Sørensen, H. 2003: A new occurrence of gabbro in the Oslo rift, South Norway. *Norges geologiske undersøkelse Bulletin 441,* 33-38.

Petersen, N.W. & Sørensen, H. 1997: A new occurrence of porphyritic syenite in the Oslo igneous province, southeast Norway. *Norsk Geologisk Tidsskrift 77*, 123–136.

Ramberg, I.B. & Larsen, B.T. 1978: Tectonomagmatic evolution. In: Dons, J.A. & Larsen, B.T. (eds.): The Oslo Paleorift. A review and guide to excursions. *Norges geologiske undersøkelse Bulletin 337,* 55-73.

Sundvoll, B. 1995: The rhomb-porphyry dyke intrusions in the Oslo Rift: Aspects of magmatectonic evolution. In: Sundvoll, B. 1995: *Magmatic and tectonic aspects of rift evolution: The Oslo (paleo-) rift.* Dr. Philos. thesis, Univ. of Oslo.

Yegorov, D.G., Korobeinikov, A.N. & Dubrovskii, M.I. 1998: CHEMPET – Calculation for the chemical systematics of igneous rocks based on the CIPW norm. *Computers & Geosciences 24,* 1-5.

Wood, D.A. 1979: A variably veined suboceanic mantle – Genetic significance for mid-ocean ridge basalts from geochemical evidence. *Geology 7,* 499–503.